# Axisymmetric Motion of a Proposed Generalized Non-Newtonian Fluid Model with Shear-dependent Viscoelastic Effects

Fernando Carapau, Paulo Correia, Luís M. Grilo and Ricardo Conceição

***Abstract*—Three-dimensional numerical simulations of non-Newtonian fluid flows are a challenging problem due to the particularities of the involved differential equations leading to a high computational effort in obtaining numerical solutions, which in many relevant situations becomes infeasible. Several models has been developed along the years to simulate the behavior of non-Newtonian fluids together with many different numerical methods. In this work we use a one-dimensional hierarchical approach to a proposed generalized third-grade fluid with shear-dependent viscoelastic effects model. This approach is based on the Cosserat theory related to fluid dynamics and we consider the particular case of flow through a straight and rigid tube with constant circular cross-section. With this approach, we manage to obtain results for the wall shear stress and mean pressure gradient of a real three-dimensional flow by reducing the exact three-dimensional system to an ordinary differential equation. This one-dimensional system is obtained by integrating the linear momentum equation over the constant cross-section of the tube, taking a velocity field approximation provided by the Cosserat theory. From this reduced system, we obtain the unsteady equations for the wall shear stress and mean pressure gradient depending on the volume flow rate, Womersley number, viscoelastic coefficients and the flow index over a finite section of the tube geometry. Attention is focused on some numerical simulations for constant and non-constant mean pressure gradient using a Runge-Kutta method.**

***Index Terms*—One-dimensional model, generalized third-grade model, shear-thickening fluid, shear-thinning fluid, Cosserat theory.**

## I. Introduction

In the last seventy years, the mathematical models related to non-Newtonian fluids have been studied extensively due to their relevance in several physical, biological, engineering and industrial applications (see e.g. Truesdell and Noll [1], Schowalter [2], and Bird et al. [3]). Amongst the many models that have been used in the scientific literature in recent decades to describe the behavior of the non-Newtonian fluids, the models associated with fluids of differential type of complexity $n$ (see Rivlin and Ericksen [4]) have received special attention. Fluids of second- and third-grade, which form a subclass of these general fluids of differential type, have been studied under different geometries and perspectives of flow situations in last years. This work deals with fluids of third-grade. Taking into account the work of Truesdell and Noll [1], we consider the constitutive equation for viscoelastic fluids of differential type (also called Rivlin-Ericksen fluids) with complexity $n = 3$, i.e., fluids of third-grade, given by

$$\mathbf{T} = -p\mathbf{I} + \mathbf{T}_E, \tag{1}$$

where

$$\begin{aligned}\mathbf{T}_E = {} & \mu\mathbf{A}_1 + \alpha_1\mathbf{A}_2 + \alpha_2\mathbf{A}_1^2 + \beta_1\mathbf{A}_3 \\ & + \beta_2(\mathbf{A}_1\mathbf{A}_2 + \mathbf{A}_2\mathbf{A}_1) + \beta_3(\mathrm{tr}\mathbf{A}_1^2)\mathbf{A}_1,\end{aligned} \tag{2}$$

where $p$ is the pressure, $-p\mathbf{I}$ is the spherical part of the stress due to the constraint of incompressibility, $\mu$ is the constant viscosity of the fluid, "tr" is the trace of the tensor $\mathbf{A}_1^2$, and $\alpha_1$, $\alpha_2$, $\beta_1$, $\beta_2$, $\beta_3$ are the normal stress coefficients – also called viscoelastic parameters. The kinematical first three Rivlin-Ericksen tensors $\mathbf{A}_1$, $\mathbf{A}_2$ and $\mathbf{A}_3$ are defined through (see Rivlin and Ericksen [4])

$$\mathbf{A}_1 = \nabla\vartheta + \big(\nabla\vartheta\big)^T, \tag{3}$$

$$\mathbf{A}_2 = \frac{d}{dt}\big(\mathbf{A}_1\big) + \mathbf{A}_1\nabla\vartheta + \big(\nabla\vartheta\big)^T\mathbf{A}_1, \tag{4}$$

and

$$\mathbf{A}_3 = \frac{d}{dt}\big(\mathbf{A}_2\big) + \mathbf{A}_2\nabla\vartheta + \big(\nabla\vartheta\big)^T\mathbf{A}_2, \tag{5}$$

where[1] $\vartheta(\mathbf{x},t) = \vartheta_i\mathbf{e}_i$ is the three-dimensional velocity field of the fluid, $\nabla\vartheta$ is the spatial velocity gradient, $\big(\nabla\vartheta\big)^T$ is the transpose of $\nabla\vartheta$ and $\frac{d}{dt}(\cdot)$ denotes the material time derivative, given by

$$\frac{d}{dt}\big(\,\cdot\,\big) = \frac{\partial}{\partial t}\big(\,\cdot\,\big) + \vartheta\cdot\nabla(\cdot). \tag{6}$$

Considering equations (1) and (2) with $\alpha_1 = \alpha_2 = \beta_1 = \beta_2 = \beta_3 = 0$, we recover the constitutive equation related to Newtonian fluids. When $\beta_1 = \beta_2 = \beta_3 = 0$ we recover the constitutive equation related to second-grade fluids. In both cases, there is a vast specialized scientific literature under different theoretical and numerical approaches. Thus, moving from a Newtonian fluid to a second-grade fluid and then to a third-grade fluid by adding new terms to the constitutive equation raises the difficulty of the problem to a higher

Manuscript received December 28, 2016; revised June 01, 2017. This work has been partially supported by Centro de Investigação em Matemática e Aplicações (CIMA) through the grant UID/MAT/04674/2013 of FCT-Fundação para a Ciência e a Tecnologia.

Fernando Carapau (corresponding author) and Paulo Correia are Auxiliary Professors at the Departamento de Matemática and CIMA, Universidade de Évora, Rua Romão Ramalho, 59, 7000-651, Évora, Portugal (e-mail: flc@uevora.pt (Fernando Carapau), pcorreia@uevora.pt (Paulo Correia)).

Ricardo Conceição is PhD. student from the Renewable Energies Chair, Universidade de Évora, Rua Romão Ramalho, 59, 7000-651, Évora, Portugal (e-mail: rfc@uevora.pt (Ricardo Conceição)).

Luís M. Grilo is Auxiliar Professor at the Unidade Departamental de Matemática e Física and CMAT-FCT-UNL, Instituto Politécnico de Tomar, Quinta do Contador, Estrada da Serra, 2300-313 Tomar, Portugal (e-mail:lgrilo@ipt.pt).

[1]Let $\mathbf{x} = (x_1, x_2, x_3)$ be the rectangular space cartesian coordinates (for convenience we set $x_3 = z$), $t$ is the time variable and $\mathbf{e}_i$ are the associated unit basis vectors. In the sequel, latin indices take the values $1,2,3$; greek indices $1,2$, and the usual summation convention is employed over a repeated index.

level both in theoretical and numerical point of view. The thermodynamic issues of the fluids related to the constitutive equation (1) with constraint (2) had been studied in detail by Fosdick and Rajagopal [5], who showed that if the fluid is to be compatible with thermodynamics in the sense that all motions of the fluid meet the Clausius-Duhem inequality and the assumption that the specific Helmholtz free energy of the fluid is a minimum in equilibrium, then

$$\mu \geqslant 0, \quad \alpha_1 \geqslant 0, \quad |\,\alpha_1+\alpha_2\,| \leqslant \sqrt{24\mu\beta_3} \tag{7}$$

and

$$\beta_1=\beta_2=0, \quad \beta_3 \geqslant 0. \tag{8}$$

Furthermore, when the inequalities are strict the fluid is asymptotically at rest, i.e., the rest state is asymptotically stable. A detailed discussion about conditions $(7)-(8)$ can be found in the works of Fosdick and Rajagopal [5], and Dunn and Rajagopal [6]. Using (1) with (2) and $(7)-(8)$ Fosdick and Rajagopal [5] showed that for an incompressible thermodynamically compatible fluid of third-grade the constitutive equation becomes

$$\mathbf{T}=-p\mathbf{I}+\Big(\mu+\beta_3(\mathrm{tr}\mathbf{A}_1^2)\Big)\mathbf{A}_1+\alpha_1\mathbf{A}_2+\alpha_2\mathbf{A}_1^2, \tag{9}$$

where the quantity inside big parenthesis can be thought of as an effective shear-dependent viscoelasticity (see Mansutti and Rajagopal [7] and Mansutti et al. [8]), which is a relevant feature in many real fluids. Therefore, in order to be able to obtain the shear-thinning or shear-thickening behavior of the flow, we propose a specific modified constitutive equation for a third-grade fluid, given by

$$\mathbf{T}=-p\mathbf{I}+\Big(\mu+\beta_3(\mathrm{tr}\mathbf{A}_1^2)\Big)^{n-1}\mathbf{A}_1+\alpha_1\mathbf{A}_2+\alpha_2\mathbf{A}_1^2, \tag{10}$$

where the positive parameter $n$ is called the flow index. When $n<1$, the fluid presents a shear-thinning behavior and a shear-thickening behavior when $n>1$. Moreover, if $n=2$ we recover the constitutive equation (9) which is associated with the shear-thickening case. The constitutive equation (9) can also be considered as a generalization of the standard second-grade fluid model, with an effective viscosity

$$\mu_{sg}=\mu+\beta_3(\mathrm{tr}\mathbf{A}_1^2). \tag{11}$$

The standard second-grade fluid, given by (9) with $\beta_3=0$, was studied by Carapau and Sequeira [9], [10] and by Carapau [11], [12], [13] and [14] in different geometries, and different types of analysis. In particular a study related to numerical simulations of perturbed flows and swirling motion was developed. Moreover, equation (10) can be considered as an extension of a generalized second-grade fluid model (see for example Carapau et al. [15]) with shear-dependent viscoelasticity given by

$$\mu(|\dot{\gamma}|)=\Big(\mu+\beta_3(\mathrm{tr}\mathbf{A}_1^2)\Big)^{n-1}. \tag{12}$$

The case of the generalized second-grade fluid model obtained from (10) with shear-dependent viscosity of the power law type, i.e.,

$$\mu(|\dot{\gamma}|)=\mu|\dot{\gamma}|^{n-1}, \quad \dot{\gamma}=\sqrt{\frac{1}{2}\mathbf{A}_1:\mathbf{A}_1}, \tag{13}$$

where $\dot{\gamma}$ is a scalar measure of the rate of shear, was studied by Carapau et al. [15]. In this work, we want to study the flow model associated with the constitutive law proposed in (10). The case $\alpha_1=\alpha_2=0$ in (10) was studied by Carapau et al. [16], and this work is an extension of the referenced proceeding. The numerical simulation of this kind of flow can be relevant in several physical, biological, engineering and industrial applications. The mathematical three-dimensional study associated with the constitutive equation (10) relating to an incompressible fluid is a complex and difficult problem, and computationally demanding. A possible simplification to the three-dimensional model (10) for an incompressible fluid inside a domain is to consider the evolution of average flow quantities using simpler one-dimensional models. Usually, in the case of laminar flow in a tube, the classical one-dimensional models are obtained by imposing additional assumptions and integrating both the equations of conservation of linear momentum and mass over the cross section of the tube. Here, we introduce an alternative one-dimensional model based on the hierarchical director approach (also called Cosserat theory) related to fluid dynamics developed by Caulk and Naghdi [17]. This hierarchical director theory consists in integrating the linear momentum equation over the constant circular cross-section of the tube, where the three-dimensional velocity field $\vartheta(\mathbf{x},t)=\vartheta_i\mathbf{e}_i$ is approximated by the Cosserat theory as follows

$$\vartheta=\mathbf{v}+\sum_{N=1}^{k}x_{\theta_1}\ldots x_{\theta_N}\mathbf{W}_{\theta_1\ldots\theta_N}, \tag{14}$$

with

$$\mathbf{v}=v_i(z,t)\,\mathbf{e}_i, \quad \mathbf{W}_{\theta_1\ldots\theta_N}=W^i_{\theta_1\ldots\theta_N}(z,t)\,\mathbf{e}_i. \tag{15}$$

In condition (14), $\mathbf{v}$ denotes the velocity along the axis of symmetry $z$ at time $t$, $x_{\theta_1}\ldots x_{\theta_N}$ are the polynomial weighting functions with order $k$, and the vectors $\mathbf{W}_{\theta_1\ldots\theta_N}$ are the director velocities which are symmetric with respect to their indices. We remark that the number $k$ identifies the order in the hierarchical theory and is related to the number of directors. In some applications these director velocities are associated with specific physical characteristics of the fluid. Considering the velocity field approximation (14) with nine-directors, i.e., $k=3$ in (14) we can predict some of the main properties of the three-dimensional fluid problem. In particular, some advantages of applying the Cosserat theory are: the theory incorporates all components of the linear momentum equation; it is a hierarchical theory, allowing to increase the accuracy of the model; there is no need to include extra assumptions to close the system; the material invariance principle is satisfied at each order and the wall shear stress enters directly in the formulation as a dependent variable. A detailed discussion about the Cosserat theory related to fluid dynamics can be found in Caulk and Naghdi [17], Green and Naghdi [18], [19] and Green et al. [20]. This Cosserat theory approach was validated on the special case of a straight tube of constant circular cross-section for Newtonian fluids (see Caulk and Naghdi [17]) and for non-Newtonian fluids (see Carapau and Sequeira [9], [21]). Moreover, this theory was validated in the case of a linearly tapered tube for non-Newtonian fluids (see Carapau [14]). The steady case for swirling motion was studied and validated for a straight tube of constant circular cross-section for Newtonian fluids (see Caulk and Naghdi [17]). Regarding Carapau and Sequeira [21], the authors considered for blood

flow the following constitutive equation

$$\mathbf{T} = -p\mathbf{I} + \mu(|\dot{\gamma}|)\mathbf{A}_1, \tag{16}$$

where $\mu(|\dot{\gamma}|)$ is the shear-dependent viscosity function. It is known that in small vessels, blood exhibits non-Newtonian phenomenon due to shear thinning-viscosity and viscoelasticity effects. In the mentioned work, numerical results were presented with the viscosity function given by both a power law type (13) and a Carreau-Yasuda law type, i.e.,

$$\mu(|\dot{\gamma}|) = \mu_\infty + \frac{\mu_0 - \mu_\infty}{(1+k^2|\dot{\gamma}|^2)^{(1-n)/2}}, \tag{17}$$

where $k$ is a positive material constant, $\mu_0$ and $\mu_\infty$ are asymptotic viscosities. In particular, the power law type solution, found using the Cosserat theory, was compared with the exact solution (see Bird et al. [3]) and it was found quantitative agreement for the blood flow index.

The aim of the present work is to apply the nine-directors theory to the proposed constitutive equation (10) in order to obtain the unsteady equations for the wall shear stress and mean pressure gradient both depending on the volume flow rate, Womersley number, viscoelastic coefficients and flow index, over a finite section of the tube geometry with constant circular cross-section. Attention is focused on some numerical simulation for constant and non-constant mean pressure gradient using a Runge-Kutta method to solve the differential equation.

## II. Equations of Motion

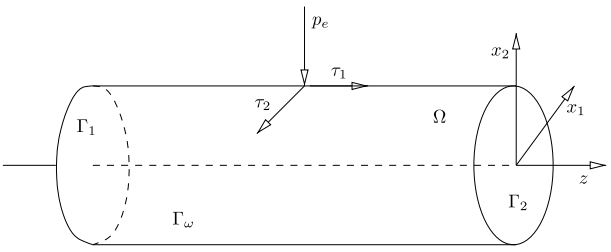


Fig. 1. Fluid domain $\Omega$ with normal and tangential components of the surface traction vector $p_e$ and $\tau_1$, $\tau_2$ with constant circular cross-section along the axis of symmetry $z$. The boundary $\partial\Omega$ is composed by the proximal cross-section $\Gamma_1$, by the distal cross-section $\Gamma_2$ and by the lateral wall of the tube $\Gamma_w$.

Let us consider a homogeneous fluid moving within a straight, rigid and impermeable tube $\Omega$ with constant circular cross-section contained in $\mathbb{R}^3$ (see Fig. 1), where the constant surface function $\phi = cts$ is related to the cross-section of the tube by

$$\phi^2 = x_1^2 + x_2^2. \tag{18}$$

The three-dimensional equations governing the axisymmetric motion of an incompressible third-grade fluid related to the constitutive equation (10), without body force, is given in $\Omega \times (0,T)$ by

$$\begin{cases} \rho\Big(\dfrac{\partial \vartheta}{\partial t} + \vartheta \cdot \nabla\vartheta\Big) = \nabla \cdot \mathbf{T}, \\ \nabla \cdot \vartheta = 0, \\ \mathbf{T} = -p\mathbf{I} + \Big(\mu + \beta_3(\mathrm{tr}\mathbf{A}_1^2)\Big)^{n-1}\mathbf{A}_1 + \alpha_1\mathbf{A}_2 + \alpha_2\mathbf{A}_1^2, \\ \mathbf{t}_w = \mathbf{T}\cdot\eta, \end{cases} \tag{19}$$

where equation $(19)_1$ represents the balance of linear momentum and $\rho$ is the constant fluid density. Equation $(19)_2$ defines the incompressibility condition, equation $(19)_3$ is the proposed constitutive equation (10) and in equation $(19)_4$, $\mathbf{t}_w$ denotes the stress vector on the surface with outward unit normal $\eta$ given by

$$\eta = \frac{x_1}{\phi}\mathbf{e}_1 + \frac{x_2}{\phi}\mathbf{e}_2. \tag{20}$$

Since equation (18) defines a material surface, the velocity field $\vartheta$ must satisfy the kinematic condition

$$\begin{aligned} \frac{d}{dt}\big(\phi^2 - x_1^2 - x_2^2\big) &= \frac{\partial}{\partial t}\big(\phi^2 - x_1^2 - x_2^2\big) \\ &\quad + \vartheta \cdot \nabla\big(\phi^2 - x_1^2 - x_2^2\big) = 0, \end{aligned}$$

i.e.,

$$x_1\vartheta_1 + x_2\vartheta_2 = 0, \tag{21}$$

on the boundary (18). Averaged quantities such as volume flow rate and pressure are needed to study one-dimensional models. Consider $S(z,t)$ a generic axial section of the tube at time $t$ defined by the spatial variable $z$, bounded by the circle defined by (18), and let $A(z,t)$ be the area of this section. Then, the volume flow rate $Q$ and the pressure $\bar{p}$ are defined, respectively, by

$$Q(z,t) = \int_{S(z,t)} \vartheta_3(x_1,x_2,z,t)da \tag{22}$$

and

$$\bar{p}(z,t) = \frac{1}{A(z,t)}\int_{S(z,t)} p(x_1,x_2,z,t)da. \tag{23}$$

Using the directors approach (14) with $k=3$, it follows from Caulk and Naghdi [17] that the approximation of the velocity field with nine-directors is given by

$$\begin{aligned} \vartheta(\mathbf{x},t) &= \Big[x_1(\xi + \sigma(x_1^2+x_2^2)) - x_2(\omega + \psi(x_1^2+x_2^2))\Big]\mathbf{e}_1 \\ &\quad + \Big[x_1(\omega + \psi(x_1^2+x_2^2)) + x_2(\xi + \sigma(x_1^2+x_2^2))\Big]\mathbf{e}_2 \\ &\quad + \Big[v_3 + \gamma(x_1^2+x_2^2)\Big]\mathbf{e}_3, \end{aligned} \tag{24}$$

where $\xi, \omega, \gamma, \sigma, \psi$ are scalar functions of the spatial variable $z$ and time $t$. The physical significance of these scalar functions is the following: $\gamma$ is related to transverse shearing motion, $\omega$ and $\psi$ are related to rotational motion (also called swirling motion) about $\mathbf{e}_3$, while $\xi$ and $\sigma$ are related to transverse elongation. We use nine-directors because it is the minimum number for which the incompressibility condition and the kinematic boundary conditions on the lateral surface of the tube are satisfied pointwise. Using the

velocity approach (24), the kinematic condition (21) on the lateral boundary reduces to

$$-\phi^2(\xi+\phi^2\sigma)=0 \tag{25}$$

and the incompressibility condition given by equation $(19)_2$ becomes

$$(v_3)_z+2\xi+(x_1^2+x_2^2)(\gamma_z+4\sigma)=0, \tag{26}$$

where the subscripted variable denotes partial differentiation. For equation (26) to hold at every point in the fluid, the velocity coefficients must satisfy the separate conditions

$$(v_3)_z+2\xi=0, \quad \gamma_z+4\sigma=0. \tag{27}$$

Hence the boundary condition (21) and the incompressiblity condition given by equation $(19)_2$ are satisfied exactly by the velocity field (24) if we impose the conditions (25) and (27). On the wall boundary of the rigid tube we impose a no-slip boundary condition requiring that the velocity field (24) vanishes identically on the surface (18). Thus, it follows that

$$\xi+\phi^2\sigma=0, \quad \omega+\phi^2\psi=0, \quad v_3+\phi^2\gamma=0. \tag{28}$$

Therefore, equation (25) is satisfied identically and the two incompressiblity conditions (27) can be rewritten as

$$(v_3)_z+2\xi=0, \quad (\phi^2 v_3)_z=0. \tag{29}$$

Considering the flow in a rigid tube with constant circular cross-section given by surface (18) without swirling motion (i.e., $\omega=\psi=0$), and conditions (22), (24), (28) and (29), then the volume flow rate $Q$ is just a function of time $t$, given by

$$Q(t)=\frac{\pi}{2}\,\phi^2 v_3(z,t). \tag{30}$$

Consequently, the velocity field (24) can be now rewritten as

$$\vartheta(\mathbf{x},t)=\frac{2Q(t)}{\pi\phi^2}\Big(1-\frac{x_1^2+x_2^2}{\phi^2}\Big)\mathbf{e}_3. \tag{31}$$

It is convenient to resolve the stress vector $\mathbf{t}_w$ on the lateral surface in terms of its outward unit normal vector $\eta$ and in terms of the components of the surface traction vectors $\tau_1,\tau_2$, and $p_e$ in the form

$$\mathbf{t}_w=\tau_1\lambda-p_e\eta+\tau_2\mathbf{e}_\theta, \tag{32}$$

where $\tau_1$ is the wall shear stress, while $\lambda$ and $\mathbf{e}_\theta$ are the unit tangent vectors defined by

$$\lambda=\eta\times\mathbf{e}_\theta, \quad \mathbf{e}_\theta=(x_\alpha/\phi)\mathbf{e}_{\alpha\beta}\mathbf{e}_\beta, \tag{33}$$

with $\mathbf{e}_{11}=\mathbf{e}_{22}=0$ and $\mathbf{e}_{12}=-\mathbf{e}_{21}=1$. Using conditions (20) and (33), the expression for the stress vector (32) can be rewritten in terms of its rectangular Cartesian components as

$$\mathbf{t}_w=\frac{1}{\phi}(-p_e x_1-\tau_2 x_2)\mathbf{e}_1+\frac{1}{\phi}(-p_e x_2+\tau_2 x_1)\mathbf{e}_2+\tau_1\mathbf{e}_3. \tag{34}$$

Now, instead of the momentum equation $(19)_1$ be verified pointwise in the fluid, we impose the following integral conditions

$$\int_{S(z,t)}\Big[\nabla\cdot\mathbf{T}-\rho\Big(\frac{\partial\vartheta}{\partial t}+\vartheta\cdot\nabla\vartheta\Big)\Big]da=0, \tag{35}$$

$$\int_{S(z,t)}\Big[\nabla\cdot\mathbf{T}-\rho\Big(\frac{\partial\vartheta}{\partial t}+\vartheta\cdot\nabla\vartheta\Big)\Big]x_{\theta_1}\ldots x_{\theta_N}da=0, \tag{36}$$

where $N=1,2,3$. Using the divergence theorem and a form of Liebnitz rule, equations (35) and (36) for nine-directors, can be reduced to the following vector equations:

$$\frac{\partial\mathbf{n}}{\partial z}+\mathbf{f}=\mathbf{a} \tag{37}$$

and

$$\frac{\partial\mathbf{m}^{\theta_1\ldots\theta_N}}{\partial z}+\mathbf{l}^{\theta_1\ldots\theta_N}=\mathbf{k}^{\theta_1\ldots\theta_N}+\mathbf{b}^{\theta_1\ldots\theta_N}, \tag{38}$$

where $\mathbf{n}$, $\mathbf{k}^{\theta_1\ldots\theta_N}$, $\mathbf{m}^{\theta_1\ldots\theta_N}$ are resultant forces defined by

$$\mathbf{n}=\int_{S(z,t)}\mathbf{T}_3da, \quad \mathbf{k}^{\theta}=\int_{S(z,t)}\mathbf{T}_\theta da, \tag{39}$$

$$\mathbf{k}^{\theta\beta}=\int_{S(z,t)}\Big(\mathbf{T}_\theta x_\beta+\mathbf{T}_\beta x_\theta\Big)da, \tag{40}$$

$$\mathbf{k}^{\theta\beta\gamma}=\int_{S(z,t)}\Big(\mathbf{T}_\theta x_\beta x_\gamma+\mathbf{T}_\beta x_\theta x_\gamma+\mathbf{T}_\gamma x_\theta x_\beta\Big)da \tag{41}$$

and

$$\mathbf{m}^{\theta_1\ldots\theta_N}=\int_{S(z,t)}\mathbf{T}_3 x_{\theta_1}\ldots x_{\theta_N}da. \tag{42}$$

The quantities $\mathbf{a}$ and $\mathbf{b}^{\theta_1\ldots\theta_N}$ are inertia terms defined by

$$\mathbf{a}=\int_{S(z,t)}\rho\Big(\frac{\partial\vartheta}{\partial t}+\vartheta\cdot\nabla\vartheta\Big)da, \tag{43}$$

$$\mathbf{b}^{\theta_1\ldots\theta_N}=\int_{S(z,t)}\rho\Big(\frac{\partial\vartheta}{\partial t}+\vartheta\cdot\nabla\vartheta\Big)x_{\theta_1}\ldots x_{\theta_N}da \tag{44}$$

and $\mathbf{f}$, $\mathbf{l}^{\theta_1\ldots\theta_N}$, which arise due to surface traction on the lateral boundary, are defined by

$$\mathbf{f}=\int_{\partial S(z,t)}\mathbf{t}_w\,ds, \tag{45}$$

$$\mathbf{l}^{\theta_1\ldots\theta_N}=\int_{\partial S(z,t)}\mathbf{t}_w\,x_{\theta_1}\ldots x_{\theta_N}ds. \tag{46}$$

The equation for the mean pressure gradient and wall shear stress will be obtained using the resulting quantities from (39) to (46) on equations $(37)-(38)$. On equations $(45)-(46)$ we will apply the stress vector $\mathbf{t}_w$ given by (34).

## III. One-dimensional Results

Using the velocity field (31) and the stress vector (34) in equations (39) to (46), we can explicitly calculate the forces $\mathbf{n}$, $\mathbf{k}^{\theta_1\ldots\theta_N}$, $\mathbf{m}^{\theta_1\ldots\theta_N}$, the inertia terms $\mathbf{a}$, $\mathbf{b}^{\theta_1\ldots\theta_N}$ and the surface tractions $\mathbf{f}$, $\mathbf{l}^{\theta_1\ldots\theta_N}$. Hence, plugging these solutions into equations $(37)-(38)$ and using equation (23), we get the unsteady equation for the non-dimensional mean pressure gradient over a finite section of the tube with $z_1<z_2$, given by

$$\begin{aligned}G(t)&=\frac{\bar{p}(z_1,t)-\bar{p}(z_2,t)}{z_2-z_1}\\&=\frac{2}{3}\mathscr{W}_o^2(1+6\alpha_1)Q_t(t)+\frac{1-\Big(1+8\beta_3Q^2(t)\Big)^{n-1}}{16\beta_3^2Q^3(t)(n^2+n)}\\&\quad+\frac{(n-1)\Big(1+8\beta_3Q^2(t)\Big)^{n-1}}{2\beta_3Q(t)(n^2+n)}+\frac{4Q(t)\Big(1+8\beta_3Q^2(t)\Big)^{n-1}}{(n+1)}.\end{aligned} \tag{47}$$

We also get the unsteady equation for the non-dimensional wall shear stress

$$\tau_1(z,t) = \frac{1}{12}\mathscr{W}_o^2\left(1+24\alpha_1\right)Q_t(t) + \frac{1-\left(1+8\beta_3 Q^2(t)\right)^{n-1}}{32\beta_3^2 Q^3(t)(n^2+n)} + \frac{(n-1)\left(1+8\beta_3 Q^2(t)\right)^{n-1}}{4\beta_3 Q(t)(n^2+n)} + \frac{2Q(t)\left(1+8\beta_3 Q^2(t)\right)^{n-1}}{(n+1)}, \tag{48}$$

where $\mathscr{W}_o = \phi\sqrt{\rho\omega_0/\mu^{n-1}}$ is the Womersley number ($\omega_0$ is the characteristic frequency for unsteady flow), $\beta_3$ and $\alpha_1$ are the non-dimensional viscoelastic coefficients and $n$ is the positive flow index. In the test cases considered below we want to simulate a pulsatile flow reason why we use the dimensionless number $\mathscr{W}_o$ which is the most commonly used parameter to reflect the pulsatility of the flow. Usually the dimensionless number $\alpha_1$ is called the Weissenberg number. Taking into account the appropriate non-dimensional variables on equation (31), we obtain the non-dimensional velocity field

$$\vartheta(\mathbf{x},t) = Q(t)\left(1-(x_1^2+x_2^2)\right)\mathbf{e}_3. \tag{49}$$

In the following, for a given mean pressure gradient, we will compare the volume flow rate solution given by (47), which was obtained by the proposed generalized third-grade constitutive equation (10), with the solution

$$G(t) = \frac{2}{3}\mathscr{W}_o^2\left(1+6\alpha_1\right)Q_t(t) + 2^{\frac{3n+5}{2}}Q^n(t), \tag{50}$$

obtained by Carapau et al. [15], considering on that work the generalized second-grade constitutive equation

$$\mathbf{T} = -p\mathbf{I} + \mu|\dot{\gamma}|^{n-1}\mathbf{A}_1 + \alpha_1\mathbf{A}_2 + \alpha_2\mathbf{A}_1^2,$$

where the shear-dependent viscosity function is the type of power law given by (13). Moreover, we will illustrate the behavior of the wall shear stress (48). The time interval was set to $[0,1.5]$ in the case of constant mean pressure gradient and it was set to $[0,4]$ in the case of non-constant mean pressure gradient, and the solutions start from rest. We solve the equation (47) considering a constant mean pressure gradient $G(t) = G_0 = 1$ and a non-constant mean pressure gradient given by (see Fig. 2)

$$G(t) = 1 + \frac{\sin^2(t)}{e^t}, \tag{51}$$

which shows an interesting behavior. More specifically it shows a strong variation in the initial stage and after the initial transient phase has small fluctuations, which tend to decrease with time. Finally, we will further illustrate the behavior of the velocity field (49) by circular cross-section for specific time parameters. In Fig. 3 and Fig. 4 we can observe the behavior of the unsteady volume flow rate solution obtained using a Runge-Kutta method, with constant mean pressure gradient, for generalized third-grade fluid (47) and for generalized second-grade fluid (50) in the case of shear-thinning and shear-thickening fluid, for specific parameters. In the case of generalized third-grade fluid the volume flow rate behavior in the initial transient phase, increasing the Weissenberg number is smoother compared to the case of generalized second-grade fluid and beyond that the volume flow rate in both situations tends to converge

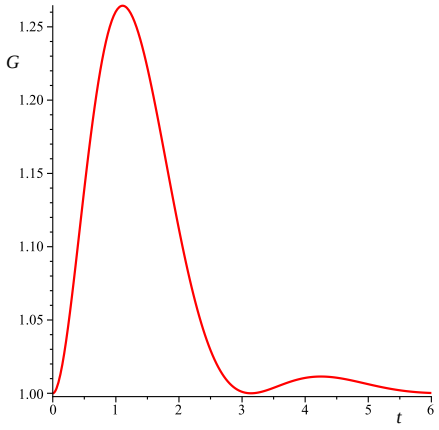


Fig. 2. Non-constant mean pressure gradient given by (51).

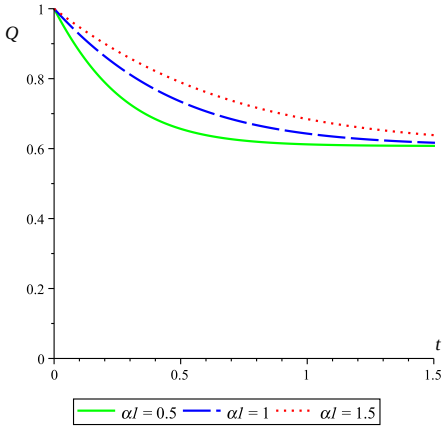


(a) Generalized third-grade fluid ($\beta_3 = 0.25$, $n = 0.5$).

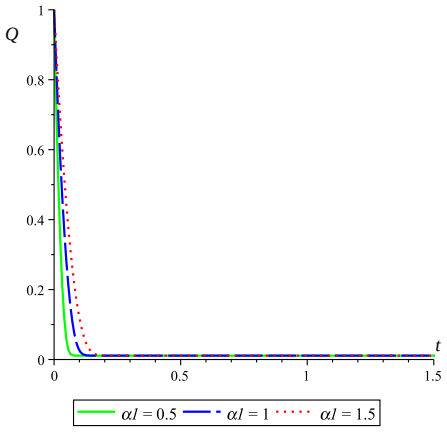


(b) Generalized second-grade fluid ($n = 0.5$).

Fig. 3. Unsteady volume flow rate (47) and (50) with constant mean pressure gradient $G(t) = G_0 = 1$ where $Q(0) = 1$, $\mathscr{W}_o = 0.3$, $\alpha_1 = 0.5$, $\alpha_1 = 1$ and $\alpha_1 = 1.5$ for shear-thinning fluid.

to the stationary solution, being this convergence more pronounced in the case of generalized second-grade fluid. Moreover, we can see from these results that increasing the value of the flow index $n$ (passing from shear-thinning to shear-thickening case) the volume flow rate solution requires less initial transient phase to achieve the stationary solution by changing the limit where we can check the influence of the parameter $\beta_3$ at the generalized third-grade fluid (47), in

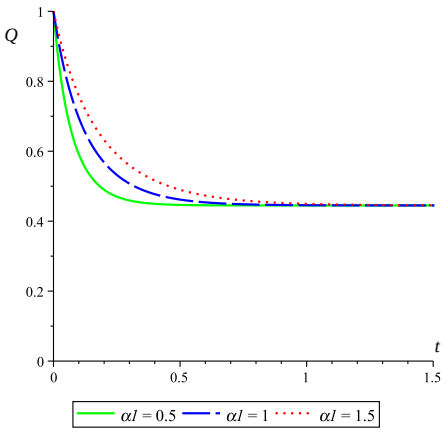


(a) Generalized third-grade fluid ($\beta_3 = 0.25$, $n = 1.5$).

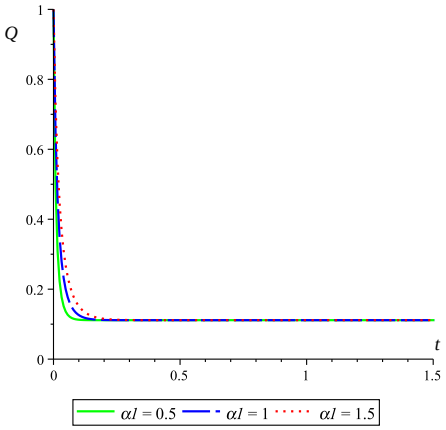


(b) Generalized second-grade fluid ($n = 1.5$).

Fig. 4. Unsteady volume flow rate (47) and (50) with constant mean pressure gradient $G(t) = G_0 = 1$ where $Q(0) = 1$, $\mathscr{W}_o = 0.3$, $\alpha_1 = 0.5$, $\alpha_1 = 1$ and $\alpha_1 = 1.5$ for shear-thickening fluid.

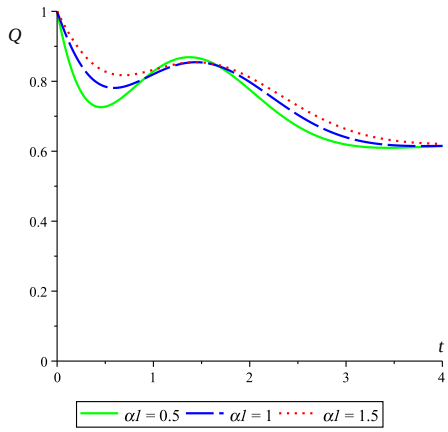


(a) Generalized third-grade fluid ($\beta_3 = 0.25$, $n = 0.5$).

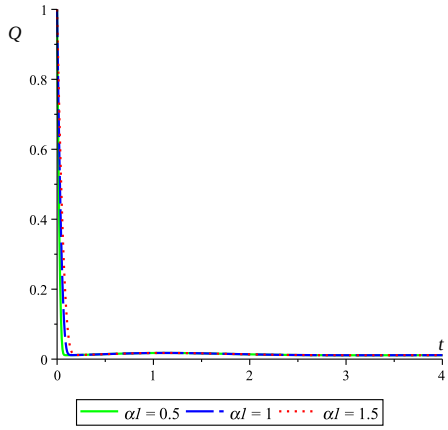


(b) Generalized second-grade fluid ($n = 0.5$).

Fig. 5. Unsteady volume flow rate (47) and (50) with non-constant mean pressure gradient (51) where $Q(0) = 1$, $\mathscr{W}_o = 0.3$, $\alpha_1 = 0.5$, $\alpha_1 = 1$ and $\alpha_1 = 1.5$ for shear-thinning fluid.

comparison with generalized second-grade fluid (50) where $\beta_3 = 0$. Also, if we are not interested in the behavior during the initial transient phase, the steady asymptotic value of the volume flow rate can be obtained directly from (47) and (50) setting $Q_t(t) = 0$, since at constant mean pressure gradient the expression $Q_t(t)$ converges to zero as $t$ goes to infinity. Now, considering the general situation of imposing a time dependent mean pressure gradient, we will see the behavior of the volume flow rate (47) and (50) obtained from different fluid models, applying a Runge-Kutta method. In this case we consider the specific mean pressure gradient (51), which presents an interesting behavior during and after the initial transient phase (see Fig. 2). In Fig. 5 and Fig. 6 it is shown the behavior of the volume flow rate obtained using a Runge-Kutta method, with non-constant mean pressure gradient (51), for generalized third-grade fluid (47) and for generalized second-grade fluid (50) in the cases of shear-thinning and shear-thickening fluid, for given parameters. In both cases, the volume flow rate tends to follow the behavior of the given non-constant mean pressure gradient. Furthermore, we can see that the behavior of the volume flow rate associated to the equation (47), compared with the one from equation (50) is smoother during the initial transient phase. In the case of shear-thickening fluid, the peaks of the graphics are less intense and the time range of the initial transient phase is smaller in comparison with the case of shear-thinning fluid. Fig. 7 and Fig. 8 displays the unsteady wall shear stress given by (48) for increasing values of the power index, passing from a shear-thinning to a shear-thickening fluid, for a given constant mean pressure gradient and non-constant mean pressure gradient given by (51), for specific fixed parameters. Here we just consider the wall shear stress related to the generalized third-grade fluid. In the case of shear-thinning fluid and during the initial transient phase the wall shear stress solution features a smooth behavior and as expected after the transient phase the solution tends to stabilize. In opposition to a shear-thinning fluid, in the case of a shear-thickening fluid we notice that the wall shear stress solution presents a very sharp behavior in the transient phase. Also, as in the case of shear-thinning fluid, the solution stabilizes to the stationary solution beyond the transient phase. We can conclude that the wall shear stress solution passing from a shear-thinning to a shear-thickening fluid, by increasing the value of the power index, presents a very sharp and strong behavior with accentuated sensitivity. Solved the one-dimensional problem we can get relevant information regarding to the three-dimensional problem, using for that the volume flow rate solution. Therefore, Fig. 9, Fig. 10, Fig. 11 and Fig. 12 illustrate the three-dimensional velocity field (49) on the tube

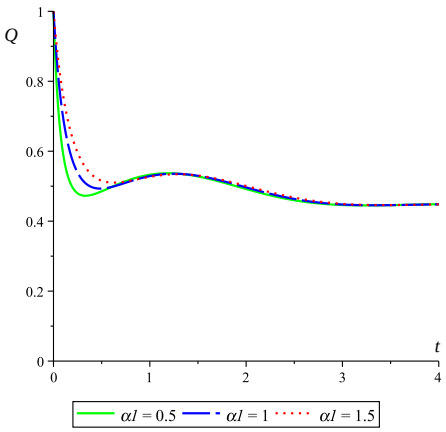


(a) Generalized third-grade fluid ($\beta_3 = 0.25$, $n = 1.5$).

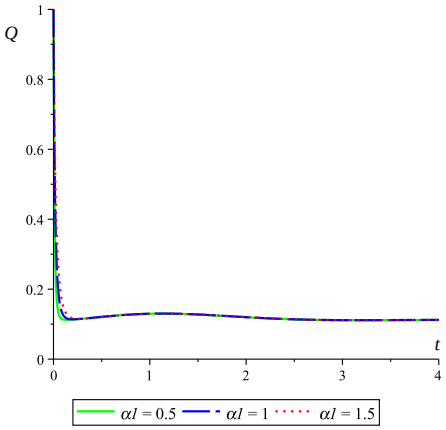


(b) Generalized second-grade fluid ($n = 1.5$).

Fig. 6. Unsteady volume flow rate (47) and (50) with non-constant mean pressure gradient (51) where $Q(0) = 1$, $\mathscr{W}_o = 0.3$, $\alpha_1 = 0.5$, $\alpha_1 = 1$ and $\alpha_1 = 1.5$ for shear-thickening fluid.

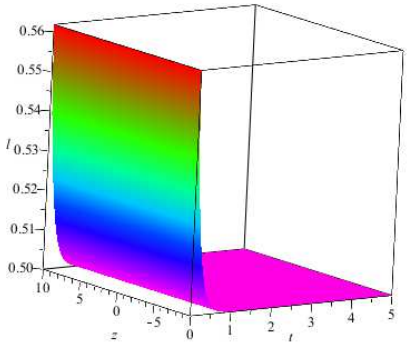


(a) Constant mean pressure gradient ($n = 0.5$).

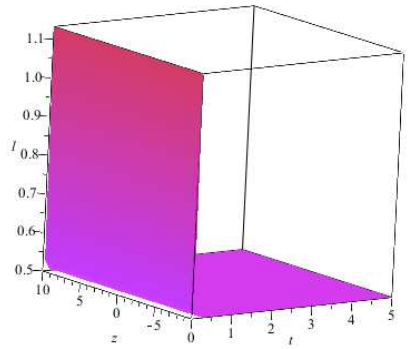


(b) Constant mean pressure gradient ($n = 1.5$).

Fig. 7. Unsteady wall shear stress (48) with constant mean pressure gradient given by $G(t) = G_0 = 1$ where $Q(0) = 1$, $\mathscr{W}_o = 0.3$, $\alpha_1 = 0.25$ and $\beta_3 = 0.25$ for shear-thinning and shear-thickening fluid.

cross-section in time, based on the one-dimensional volume flow rate solution $Q(t)$ obtained by (47) with mean pressure gradient $G(t) = G_0 = 1$ for specific parameters, in both situations of shear-dependent viscoelastic effects, i.e., shear-thinning and shear-thickening fluid. Finally, Fig. 13, Fig. 14, Fig. 15 and Fig. 16 illustrate the cross-section of the three-dimensional velocity field (49) in the case of shear-thinning and shear-thickening fluid considering specific parameters at the ordinary differential equation (47), with non-constant mean pressure gradient (51).

## IV. Perturbed flows

The theoretical study of the three-dimensional model associated to the constitutive equation (10), namely existence, uniqueness and regularity of classical and weak solutions with any $\mu, \alpha_1, \alpha_2$, $\beta_3$ and flow index $n$, still poses some difficulties. In many industrial applications involving fluid flows in specific domains it is important to determine the changes in flow characteristics induced by perturbations in the initial or boundary data, body forces or pressure drop. In fact, since it is virtually impossible to maintain an exactly constant pressure drop, one should be able to predict how much a perturbation of given magnitude in pressure drop will affect the volume flow rate. Therefore, we want to perturb the solution (47) obtained by the Cosserat theory and analyze its stability. Let us consider a uniform perturbation of magnitude $\varepsilon$. For each $\varepsilon > 0$, defining the quantities,

$$G_\varepsilon^+(t) = (1+\varepsilon)G(t), \quad G_\varepsilon^-(t) = (1-\varepsilon)G(t), \tag{52}$$

we denote by $Q_\varepsilon^+$ and $Q_\varepsilon^-$ the perturbed volume flow rates corresponding to $G_\varepsilon^+$ and $G_\varepsilon^-$, respectively. Taking into account the complexity and difficulty of the solution (47) it is not possible to deduce exact expression for the perturbed volume flow rate with constant and non-constant mean pressure gradient. However, we can compute the time evolution of the perturbation volume flow rate $Q_\varepsilon^\pm$ for both cases. Here, we just study the general case of the perturbed volume flow rate with non-constant mean pressure gradient, the case of constant mean pressure gradient being similar.

Now, considering the perturbation $G_\varepsilon^\pm = (1 \pm \varepsilon)G(t)$, where $G(t)$ is the non-constant mean pressure gradient (51), we can use the characterization of the unsteady solution (47), and explicitly compute the perturbed volume flow rate $Q_\varepsilon^\pm$, see Fig. 17, where the perturbed volume flow rate forming a strip around $Q(t)$ containing all perturbations of magnitude less or equal to $\varepsilon = 0.1$ and we realize that the stability of the solution exists and increases as the flow index increases. Fig. 18 shows the amplitude of this strip around $Q(t)$ for several values of $n$, showing that increasing the flow index $n$ reduces sensitivity to perturbations. Considering other values for $\mathscr{W}_o$,

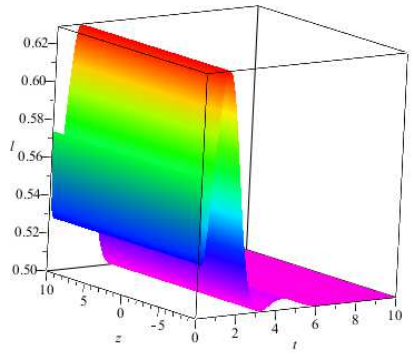

(a) Non-constant mean pressure gradient ($n = 0.5$).

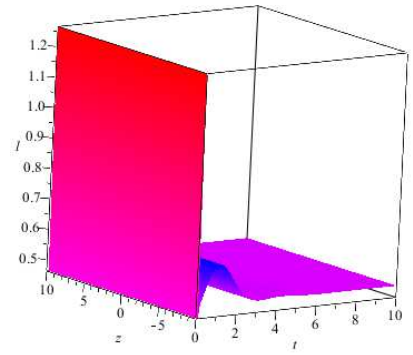

(b) Non-constant mean pressure gradient ($n = 1.5$).

Fig. 8. Unsteady wall shear stress (48) with non-constant mean pressure gradient given by (51) where $Q(0) = 1$, $\mathscr{W}_o = 0.3$, $\alpha_1 = 0.25$ and $\beta_3 = 0.25$ for shear-thinning and shear-thickening fluid.

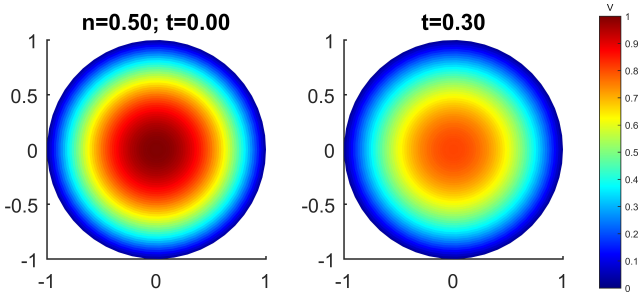


Fig. 9. Velocity field (49) where the volume flow rate is obtained by (47) with mean pressure gradient $G(t) = G_0 = 1$. In the illustration are considered the following parameters: time ($t = 0, t = 0.3$), $Q(0) = 1$, $\mathscr{W}_o = 0.3$, $\alpha_1 = 1$, $\beta_3 = 0.25$ and $n = 0.5$ (shear-thinning fluid).

$\alpha_1$, $\beta_3$ and flow index we get a similar solution behavior as shown in Fig. 17 and Fig. 18.

## V. Conclusion

The Cosserat theory approach plays an important alternative process to reduce the number of variables of a three-dimensional fluid model thus simplifying the study related to the numerical simulations in terms of computational effort. By applying this approach theory to our proposed generalized third-grade fluid model (19) with shear-dependent viscoelastic effects allowed us to obtain a one-dimensional ODE

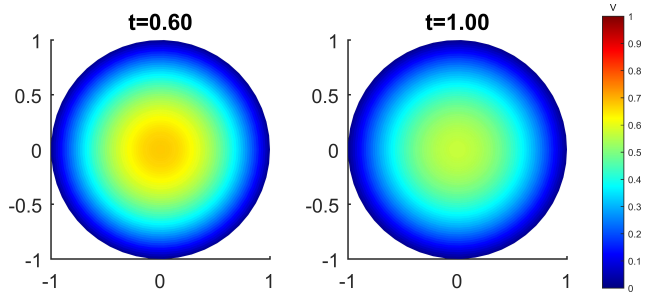


Fig. 10. Velocity field (49) where the volume flow rate is obtained by (47) with mean pressure gradient $G(t) = G_0 = 1$. In the illustration are considered the following parameters: time ($t = 0.6, t = 1$), $Q(0) = 1$, $\mathscr{W}_o = 0.3$, $\alpha_1 = 1$, $\beta_3 = 0.25$ and $n = 0.5$ (shear-thinning fluid).

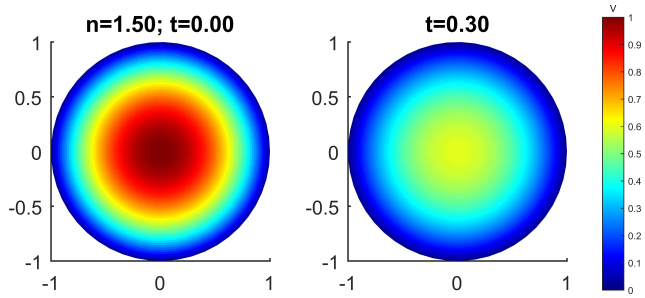


Fig. 11. Velocity field (49) where the volume flow rate is obtained by (47) with mean pressure gradient $G(t) = G_0 = 1$. In the illustration are considered the following parameters: time ($t = 0, t = 0.3$), $Q(0) = 1$, $\mathscr{W}_o = 0.3$, $\alpha_1 = 1$, $\beta_3 = 0.25$ and $n = 1.5$ (shear-thickening fluid).

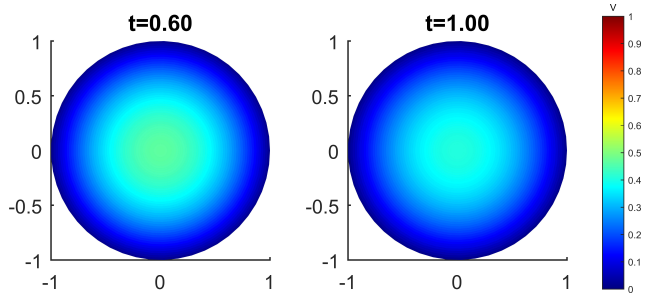


Fig. 12. Velocity field (49) where the volume flow rate is obtained by (47) with mean pressure gradient $G(t) = G_0 = 1$. In the illustration are considered the following parameters: time ($t = 0.6, t = 1$), $Q(0) = 1$, $\mathscr{W}_o = 0.3$, $\alpha_1 = 1$, $\beta_3 = 0.25$ and $n = 1.5$ (shear-thickening fluid).

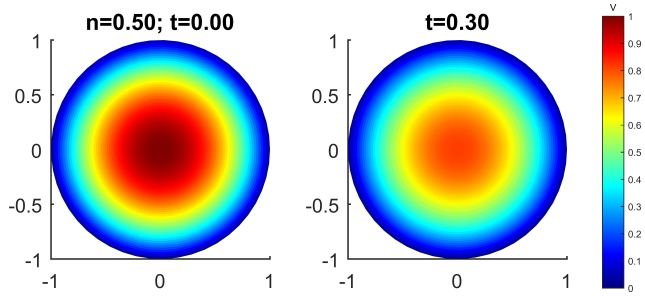


Fig. 13. Velocity field (49) where the volume flow rate is obtained by (47) with non-constant mean pressure gradient (51). In the illustration are considered the following parameters: time ($t = 0, t = 0.3$), $Q(0) = 1$, $\mathscr{W}_o = 0.3$, $\alpha_1 = 1$, $\beta_3 = 0.25$ and $n = 0.5$ (shear-thinning fluid).

system with which it was possible to obtain the unsteady equations for the wall shear stress and mean pressure gradient depending on the volume flow rate, Womersley number, viscoelastic coefficients and flow index over a finite section

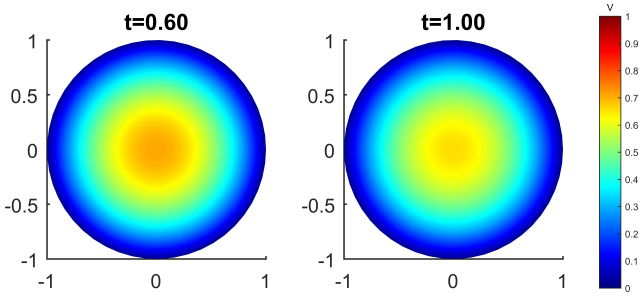


Fig. 14. Velocity field (49) where the volume flow rate is obtained by (47) with non-constant mean pressure gradient (51). In the illustration are considered the following parameters: time ($t = 0.6, t = 1$), $Q(0) = 1$, $\mathscr{W}_o = 0.3$, $\alpha_1 = 1$, $\beta_3 = 0.25$ and $n = 0.5$ (shear-thinning fluid).

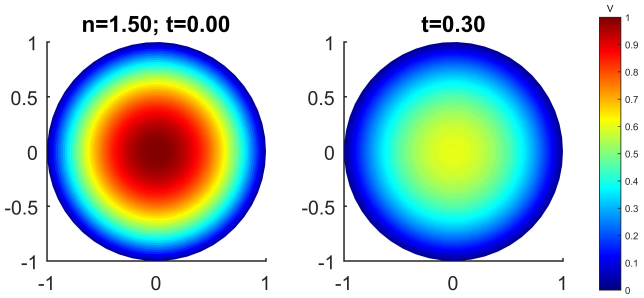


Fig. 15. Velocity field (49) where the volume flow rate is obtained by (47) with non-constant mean pressure gradient (51). In the illustration are considered the following parameters: time ($t = 0, t = 0.3$), $Q(0) = 1$, $\mathscr{W}_o = 0.3$, $\alpha_1 = 1$, $\beta_3 = 0.25$ and $n = 1.5$ (shear-thickening fluid).

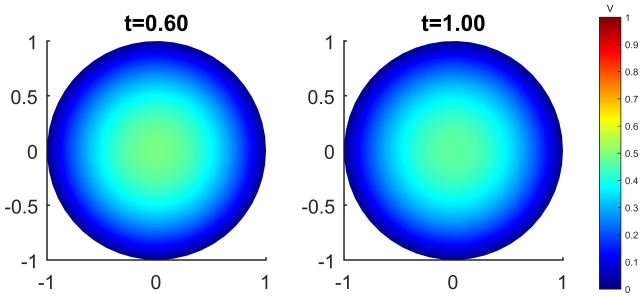


Fig. 16. Velocity field (49) where the volume flow rate is obtained by (47) with non-constant mean pressure gradient (51). In the illustration are considered the following parameters: time ($t = 0.6, t = 1$), $Q(0) = 1$, $\mathscr{W}_o = 0.3$, $\alpha_1 = 1$, $\beta_3 = 0.25$ and $n = 1.5$ (shear-thickening fluid).

of the tube with constant circular cross-section. Based on the numerical simulations here presented, we may conclude that the generalized third-grade fluid model (19) is better suited for a shear-thinning fluid that presents a smoother behavior with regard to its volume flow rate, for a given mean pressure gradient, during the initial transient phase. Also, we conducted numerical simulations of perturbed flows, providing a first step towards stability analysis of the model. Possible extensions of this work are the application of this hierarchical approach theory to the same fluid model (19) but considering a tube geometry with variable circular cross-section along the flow motion axis, and also the coupling of Cosserat models in geometrical multi-scale models.

## Acknowledgment

This work has been partially supported by Centro de Investigação em Matemática e Aplicações (CIMA) through the grant UID/MAT/04674/2013 of FCT-Fundação para a Ciência e a Tecnologia. The authors would like to thank the referees for their helpful comments to improve the paper.

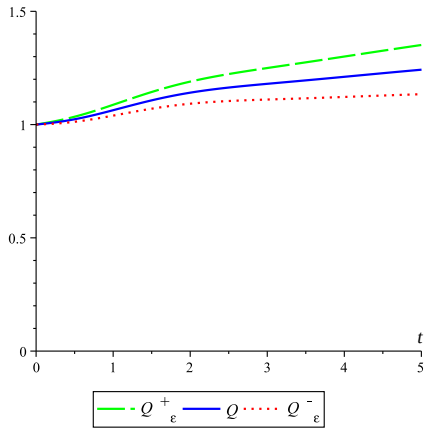


(a) Flow index $n = 0.5$.

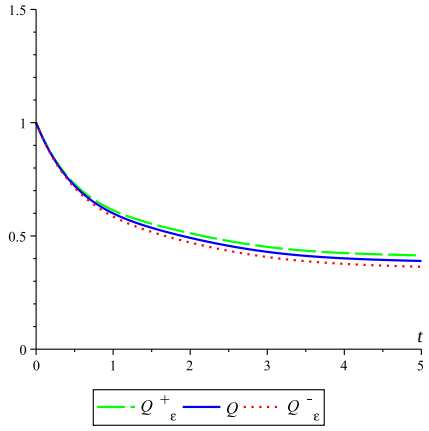


(b) Flow index $n = 1.5$.

Fig. 17. Time evolution of the unperturbed volume flow rate $Q$ and perturbed volume flow rate $Q^{\pm}_{\varepsilon}$, with magnitude $\varepsilon = 0.1$, where $Q(0) = 1$, $\mathscr{W}_o = 1$, $\alpha_1 = 1$ and $\beta_3 = 1$.

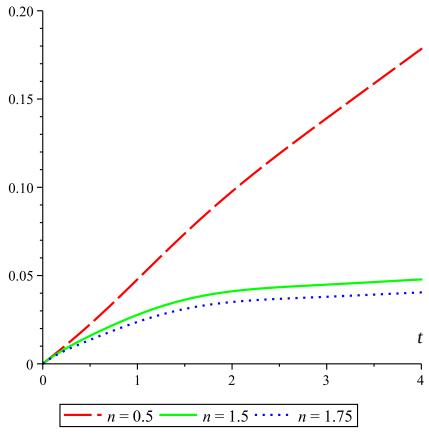


Fig. 18. Time evolution of perturbation $|Q^{+}_{\varepsilon} - Q^{-}_{\varepsilon}|$ with magnitude $\varepsilon = 0.1$, where $Q(0) = 1$, $\mathscr{W}_o = 1$, $\alpha_1 = 1$ and $\beta_3 = 1$.

## References

[1] C., Truesdell, W., Noll, *The Nonlinear Field Theories of Mechanics*, Handbuch der physik, Springer, Berlin-Heidelberg-New York, 1965.

[2] W.R., Schowalter, *Mechanics of Non-Newtonian Fluids*, Pergamon Press, Oxford, 1978.

[3] B.R., Bird, R.C., Armstrong, O., Hassager, *Dynamics of Polymeric Liquids*, **1**, 2$^{nd}$Edition, John Wiley & Sons, 1987.

[4] R.S., Rivlin, J.L., Ericksen, Stress-deformation relations for isotropic materials, *J. Rational Mech. Anal.*, **4** (1955), 323–425.
[5] R.L., Fosdick, K.R., Rajagopal, Thermodynamics and stability of fluids of third grade, *Proc. R. Soc. Lond. A.*, **339** (1980), 351–377.
[6] J.E., Dunn, K.R., Rajagopal, Fluids of differential type: critical review and thermodynamic analysis, *Int. Journal of Engineering Science*, **33** (1995), 689–729.
[7] D., Mansutti, K.R., Rajagopal, Flow of a shear thinning fluid between intersecting planes, *Int. J. Non-Linear Mech.*, **26** (5) (1991), 769–775.
[8] D., Mansutti, G., Pontrelli, K.R., Rajagopal, Steady flow of non-Newtonian fluids past a porous plate with suction or injection, *Int. J. Numer. Methods Fluids*, **17** (11) (1993), 927–941.
[9] F., Carapau, A., Sequeira, Axisymmetric motion of a second order viscous fluid in a circular straight tube under pressure gradients varying exponentially with time, *WIT Transactions on Engineering Sciences*, **52** (2006), 409–419.
[10] F., Carapau, A., Sequeira, 1D dynamics of a second-grade viscous fluid in a constricted tube, *Banach Center Publications, Inst. Math, Polish Acad. Sc.*, **81** (2008), 95–103.
[11] F., Carapau, Analysis of perturbed flows of a second-order fluid using a 1D hierarchical model, *Inter. Journal of Mathematics and Computers in Simulation*, **20** (3) (2008), 256–263.
[12] F., Carapau, Axisymmetric motion of a generalized Rivlin-Ericksen fluid with shear-dependent normal stress coefficients, *Inter. Journal of Mathematical Models and Methods in Applied Sciences*, **2** (2) (2008), 168–175.
[13] F., Carapau, Axisymmetric Swirling Motion of Viscoelastic Fluid Flow Inside a Slender surface of Revolution, *Engineering Letters*, **17** (4) (2009), 238–245.
[14] F., Carapau, 1D Viscoelastic Flow in a Circular Straight Tube with Variable Radius, *Int. J. Appl. Math. Stat.*, **19** (10) (2010), 20–39.
[15] F., Carapau, A., Sequeira, J., Janela, 1D simulations of second-grade fluids with shear-dependent viscosity, *WSEAS Transactions on Mathematics*, **6** (1) (2007), 151–158.
[16] F., Carapau, P., Correia, L.M., Grilo, Specific shear-dependent viscosity third-grade fluid model, *ICCMSE 2016, 17-24 March, Athens, Greece*, AIP Conference Proceeding, **1790**, 140008-1–140008-4; doi:10.1063/1.4968737.
[17] D.A., Caulk, P.M., Naghdi, Axisymmetric motion of a viscous fluid inside a slender surface of revolution, *Journal of Applied Mechanics*, **54** (1) (1987), 190–196.
[18] A.E., Green, P.M., Naghdi, A direct theory of viscous fluid flow in channels, *Arch. Ration. Mech. Analysis*, **86** (1) (1984), 39–63.
[19] A.E. Green, P.M., Naghdi, A direct theory of viscous fluid flow in pipes I: Basic general developments, *Phil. Trans. R. Soc. Lond. A*, **342** (1) (1993), 525–542.
[20] A.E., Green, P.M., Naghdi, M.J. Stallard, A direct theory of viscous fluid flow in pipes II: Flow of incompressible viscous fluid in curved pipes, *Phil. Trans. R. Soc. Lond. A*, **342** (1) (1993), 543–572.
[21] F., Carapau, A., Sequeira, 1D Models for Blood Flow in Small Vessels Using the Cosserat Theory, *WSEAS Transactions on Mathematics*, **5** (1) (2006), 54–62.